Complete and incomplete fusion in heavy-ion collisions

L. F. Canto, R. Donangelo, and Lia M. de Matos
Instituto de Física, Universidade Federal do Rio de Janeiro, Caixa Postale 68528, Rio de Janeiro, 21945-970, Brazil

M. S. Hussein
Instituto de Física, Universidade de São Paulo, Caixa Postale 66318, São Paulo, 05389-970, Brazil

P. Lotti
Istituto Nazionale di Fisica Nucleare, Sezione di Padova Via F. Marzolo 8, I-35131, Padova, Italy
(Received 28 July 1997)

We develop a formalism to study the influence of the breakup process of a weakly bound projectile on the complete fusion cross section. We show that the complete fusion and the resulting incomplete fusion cross sections can be expressed in terms of breakup and survival probabilities, which are evaluated with the help of appropriate polarization potentials. The effects of the finite size of the projectile and of Fermi motion are estimated. As examples, we consider light–heavy-ion collisions where threshold effects play an interesting role. [S0556-2813(98)04908-5]

PACS number(s): 25.70.Jj, 25.60.Gc

I. INTRODUCTION

The fusion of heavy ions at energies in the vicinity of the Coulomb barrier has been extensively discussed in the past several years. The question of coupled channel effects on the fusion cross section σ_F has been widely debated and a rather satisfactory picture has emerged: coupled channels enhance σ_F in the no-coupling case, regardless of the nature of the channels (inelastic or transfer) and their region of Q value.

Because of the normally large Q value of the breakup channels, their effects have usually been discussed when above barrier energies, where ''normal'' coupled channels have little effect. Breakup followed by fusion, so-called incomplete fusion (IF), competes with complete fusion (CF) (the fusion of the intact projectile) in this energy regime. This competition, owing to the effect of coupling to the breakup channel, leads to a reduction in $\sigma_{\rm CF}$.

The above scenario changes when discussing fusion of loosely bound projectiles. Even at sub-barrier energies there are important breakup coupling effects. Therefore, a real competition between ''normal'' and breakup channels arises in this case. A natural question is raised in this connection which is whether the breakup coupling results in an *increase* in the complete fusion cross section, just like the effect of the coupling to ''normal'' channels, or a *reduction*, since the incomplete fusion is operative here. The above question has recently been discussed in several papers [1–3] but a fully satisfactory answer has not yet been given. Since experimental efforts to measure σ_F for ^{11}Li on heavy target nuclei are presently underway, a better understanding of this phenomenon is clearly called for. It is the purpose of this paper to further elucidate the role of breakup coupling on heavy-ion fusion involving weakly bound two-cluster projectiles. By doing so, we may assess the findings of the above references.

Since data do exist [4] for systems such as ^{6}Li+^{12}C and ^{6}Li+^{9}Be, we shall, in the following, discuss a theoretical framework through which $\sigma_{\rm CF}$ and $\sigma_{\rm IF}$ can be calculated with the effect of breakup included. This formulation allows the projectile and/or target to break up.

II. FORMAL REACTION THEORY

A natural framework through which the questions raised in the introduction can be fully addressed is to consider the fusion of a two-cluster projectile with a target. Let us consider the collision of a projectile a with a target A and introduce the projectors $\hat{P}$, $\hat{B}$, and $\hat{R}$, acting on the full Hamiltonian H and on the total wave function Ψ. They project, respectively, the components of Ψ in the elastic channel $(\hat{P}\Psi)$, in the space of breakup states $(\hat{B}\Psi)$, and in the remaining reaction channels $(\hat{R}\Psi)$. Using these projectors, the full Schrödinger equation can be split into the coupled equations

$$\begin{aligned}(E-\hat{P}H\hat{P})\hat{P}\Psi&=(\hat{P}H\hat{R})\hat{R}\Psi+(\hat{P}H\hat{B})\hat{B}\Psi,\\(E-\hat{R}H\hat{R})\hat{R}\Psi&=(\hat{R}H\hat{P})\hat{P}\Psi+(\hat{R}H\hat{B})\hat{B}\Psi,\\(E-\hat{B}H\hat{B})\hat{B}\Psi&=(\hat{B}H\hat{P})\hat{P}\Psi+(\hat{B}H\hat{R})\hat{R}\Psi.\end{aligned}\tag{1}$$

We are interested in the case where the subspace projected by $\hat{R}$ contains a single state (or an effective state), so that $\hat{R}\Psi=\Psi_R$ and, further, that the states in the breakup channel are such that the fragments are emitted with negligible relative energy in their center of mass frame. Equations (1) then reduce to the simpler set

$$\begin{aligned}(E-H_0^{\rm opt})\Psi_0&=V_{0R}\Psi_R+V_{0B}\Psi_B,\\(E-E_R-H_R^{\rm opt})\Psi_R&=V_{R0}\Psi_0+V_{RB}\Psi_B,\\(E-E_B-H_B^{\rm opt})\Psi_B&=V_{B0}\Psi_0+V_{BR}\Psi_R.\end{aligned}\tag{2}$$

Above, $\Psi_0=\hat{P}\Psi$, $\Psi_R=\hat{R}\Psi$, $\Psi_B=\hat{B}\Psi$, E_R stands for the intrinsic energy in channel R, and E_B is given by the breakup Q value. $H_i^{\rm opt}$ refers to the no-coupling optical Hamiltonian in channel i (with an imaginary part that takes into account the loss of flux to complete fusion in that channel). In par-

ticular, the Hamiltonian $H_B^{\rm opt}$ describes the optical propagation of the two unbound clusters of the projectile c_1 and c_2 (with $c_1+c_2=a$) in the complex mean field of the target nucleus. The V's are appropriate channel-coupling potentials, assumed to be real.

It is convenient to formally eliminate the breakup channel. By inverting the last of the equations in Eq. (2), one can write

$$\Psi_B^{(+)}=(E-E_B-H_B^{\rm opt})^{-1}[V_{B0}\Psi_0^{(+)}+V_{BR}\Psi_R^{(+)}] \equiv G_B^{(+)}[V_{B0}\Psi_0^{(+)}+V_{BR}\Psi_R^{(+)}]. \quad (3)$$

Accordingly, the wave functions $\Psi_0^{(+)}$ and $\Psi_R^{(+)}$ are solutions of the equivalent two coupled equations

$$(E-H_0-V_{00}^{B\ {\rm pol}})\Psi_0=(V_{0R}+V_{0R}^{B\ {\rm pol}})\Psi_R,$$
$$(E-E_R-H_R^{\rm opt}-V_{RR}^{B\ {\rm pol}})\Psi_R=(V_{R0}+V_{R0}^{B\ {\rm pol}})\Psi_0, \quad (4)$$

where the breakup effective polarization potentials are given by

$$V_{ij}^{B\ {\rm pol}}=V_{iB}G_B^{(+)}V_{Bj}. \quad (5)$$

Above, i and j stand for the channels 0 and R.

For future use, we write below the imaginary part of $V_{ij}^{B\ {\rm pol}}$, assuming V_{iB} and V_{Bj} to be real. For this purpose, we write the propagator in the breakup channel in the form

$$G_B^{(+)}=(E-E_B-h_{c_1}^{\rm opt}-h_{c_2}^{\rm opt}+i\varepsilon)^{-1}, \quad (6)$$

where

$$h_{c_1}^{\rm opt}=K_{c_1}+U_{c_1} \quad \text{and} \quad h_{c_2}^{\rm opt}=K_{c_2}+U_{c_2} \quad (7)$$

are the optical Hamiltonians for the collision of each of the fragments with the target. We get

$${\rm Im}\{V_{ij}^{B\ {\rm pol}}\}=V_{iB}[\pi\Omega_B^{(-)}\delta(E-E_B-K_{c_1}-K_{c_2})(\Omega_B^{(-)})^\dagger + (G_B^{(+)})^\dagger {\rm Im}\{U_{c_1}+U_{c_2}\}G_B^{(+)}]V_{Bj}, \quad (8)$$

where $\Omega_B^{(-)}$ is the Møller wave operator given by

$$\Omega_B^{(-)}=1+G_B^{(-)}(U_{c_1}+U_{c_2})^\dagger. \quad (9)$$

The quantity within square brackets in Eq. (8) corresponds to the imaginary part of the Green's function associated to a non-Hermitian Hamiltonian [5], as shown in the Appendix. The first term on the right-hand side (RHS) of Eq. (8) represents the contribution of elastic breakup, whereas the second term represents inelastic breakup (or incomplete fusion, if ${\rm Im}\{U_{c_1}\}$ and ${\rm Im}\{U_{c_2}\}$ represent absorption of c_1 and c_2 into the fusion channels, as in our case here). At this stage, one should point out that the adopted form of the propagator in the breakup channel [Eqs. (6) and (7)] involves two approximations. The first is that we are neglecting final state interactions between the fragments. The second is that the target recoil is not properly taken into account. This approximation is justified when the target mass is much larger than those of the projectile fragments. In our case this condition is not fully met. As a consequence, it will be necessary to include a correction in the incomplete fusion cross section, as will be discussed in the next section.

We may now perform further reduction of Eq. (4) to obtain the effective equation for Ψ_0,

$$[E-H_0^{\rm opt}-V^{\rm pol}]\Psi_0^{(+)}=0, \quad (10)$$

where the optical Hamiltonian in the elastic channel can be written $H_0^{\rm opt}=K_0-U_0$. Above, we have introduced the total polarization potential $V^{\rm pol}$

$$V^{\rm pol}=V_{00}^{B\ {\rm pol}}+V_{00}^{R\ {\rm pol}} \quad (11)$$

including the contribution from the coupling to the R channel

$$V_{00}^{R\ {\rm pol}}=(V_{0R}+V_{0R}^{B\ {\rm pol}})G_R^{(+)}(V_{R0}+V_{R0}^{B\ {\rm pol}}). \quad (12)$$

We have used the propagator

$$G_R^{(+)}=(E-E_R-H_R^{\rm opt}-V_{RR}^{B\ {\rm pol}}+i\varepsilon)^{-1}, \quad (13)$$

where $H_R^{\rm opt}=K_R-U_R$ is the optical Hamiltonian for a collision initiated in channel R.

The total reaction cross section is then given by [5]

$$\sigma_r=\frac{k}{E}\langle\Psi_0^{(+)}|-{\rm Im}\{U_0+V_{00}^{B\ {\rm pol}}+V_{00}^{R\ {\rm pol}}\}|\Psi_0^{(+)}\rangle. \quad (14)$$

The reactive content of $V_{00}^{B\ {\rm pol}}$ is elastic breakup and incomplete fusion [see Eq. (8)]. The reactive content of $V_{00}^{R\ {\rm pol}}$ is more complicated; complete fusion through the R space plus higher-order processes that can be described in details by evaluating its imaginary part. We have

$${\rm Im}\{V_{00}^{R\ {\rm pol}}\}=V_{0R}[\pi\Omega_R^{(-)}\delta(E-E_R-K_R)\Omega_R^{(-)\dagger} - G_R^{(+)\dagger}\ {\rm Im}\{U_R+V_{RR}^{R\ {\rm pol}}\}G_R^{(+)}]V_{R0}. \quad (15)$$

We define complete fusion $\sigma_{\rm CF}$ as that part of σ_r which contains explicit reference to ${\rm Im}\{U_0\}$ and ${\rm Im}\{U_R\}$. We also define incomplete fusion $\sigma_{\rm IF}$ as that which contains reference to ${\rm Im}\{U_{c_1}\}$ or ${\rm Im}\{U_{c_2}\}$. The rest of the total reaction cross section is formed by elastic breakup to three-body states $\sigma_{{\rm el}\ B}$ and the inelastic excitation to states in the R space $\sigma_{\rm in}$. Thus within our model, we write

$$\sigma_r=\sigma_{{\rm el}\ B}+\sigma_{\rm in}+\sigma_{\rm CF}+\sigma_{\rm IF}. \quad (16)$$

The elastic breakup cross section $\sigma_{{\rm el}\ B}$ is given by

$$\sigma_{{\rm el}\ B}=\frac{k}{E}\langle\Psi_0^{(+)}|V_{0B}\Omega_B^{(-)} \times\delta(E-E_B-K_{c_1}-K_{c_2})\Omega_B^{(-)\dagger}V_{B0}|\Psi_0^{(+)}\rangle. \quad (17)$$

The inelastic cross section is

$$\sigma_{\rm in}=\frac{k}{E}\langle\Psi_0^{(+)}|V_{0R}\Omega_R^{(-)}\delta(E-E_R-K_R)\Omega_R^{(-)\dagger}V_{R0}|\Psi_0^{(+)}\rangle, \quad (18)$$

where the Møller operator $\Omega_R^{(-)}$, which contains the effect of breakup on the distortion of the R channels, has a definition similar to Eq. (9). The complete fusion cross section is

$$\sigma_{\rm CF}=\frac{k}{E}\{\langle\Psi_0^{(+)}|{\rm Im}\{U_0\}|\Psi_0^{(+)}\rangle+\langle\Psi_R^{(+)}|{\rm Im}\{U_R\}|\Psi_R^{(+)}\rangle\}. \tag{19}$$

This cross section will be considered in detail in the next section.

Finally, the incomplete fusion cross section can be written

$$\sigma_{\rm IF}=\sigma_{\rm IF\,0}+\sigma_{\rm IF\,R}, \tag{20}$$

where

$$\sigma_{\rm IF\,0}=\frac{k}{E}\langle\Psi_0^{(+)}|V\hat{B}G_B^{(+)\dagger}\ {\rm Im}\{U_{c_1}+U_{c_2}\}G_B^{(+)}\hat{B}V|\Psi_0^{(+)}\rangle \tag{21}$$

and

$$\sigma_{\rm IF\,R}=\frac{k}{E}\langle\Psi_R^{(+)}|V\hat{B}G_{B-R}^{(+)\dagger}\ {\rm Im}\{U_{c_1-R}+U_{c_2-R}\}G_{B-R}^{(+)}V_{BR}|\Psi_R^{(+)}\rangle. \tag{22}$$

The contributions $\sigma_{\rm IF\,0}$ and $\sigma_{\rm IF\,R}$ differ in the order of the breakup process leading to the fusing fragment. In the first term, breakup is reached through the coupling with the entrance channel. The second term is more complicated. There, the breakup channel is fed from an inelastic state, excited from the entrance channel in a previous step. Accordingly, it may involve a different Green's function and different optical potentials. To emphasize these points, we use the notations $G_{B\,R}^{(+)}$, $U_{c_1\,R}$, and $U_{c_2\,R}$.

III. THEORY OF COMPLETE FUSION AND INCOMPLETE FUSION REACTIONS

In the previous section we developed a general formalism to treat elastic and inelastic scattering together with complete and incomplete fusion on the same grounds. Here, we develop in detail approximate expressions to evaluate the complete and the incomplete fusion cross sections.

A. The complete fusion cross section

The complete fusion cross section is given by Eq. (19). In this equation the wave functions Ψ_0 and Ψ_R are solutions of the full coupled-channel problem [Eqs. (1)]. Therefore, they are influenced by one another and also by the breakup channel. It is well known that in the absence of the breakup channel the coupling tends to enhance the fusion cross section at sub-barrier energies. However, the coupling to breakup introduces additional complications, which should be considered with care. To simplify the discussion, let us fist consider $\langle\Psi_0^{(+)}|U_0|\Psi_0^{(+)}\rangle$ in the absence of the inelastic channel R. By expanding in partial waves, we can write for the fusion cross section the usual expression

$$\sigma_F=\frac{\pi}{k^2}\sum_{\ell=0}^{\infty}(2\ell+1)T_\ell, \tag{23}$$

$$T_\ell=\frac{8\mu}{k\hbar^2}\int_0^\infty dr|\Psi_{0,\ell}(k,r)|^2{\rm Im}\{U_0(r)\}, \tag{24}$$

where $\Psi_{0,\ell}(k,r)$ is the radial elastic wave function that satisfies the equation

$$\left[-\frac{\hbar^2}{2\mu}\left(\frac{d^2}{dr^2}-\frac{\ell(\ell+1)}{r^2}\right)+U_0+V_{00,\ell}^{B\ {\rm pol}}-E\right]\Psi_{0,\ell}(k,r)=0. \tag{25}$$

To find $\Psi_{0,\ell}(k,r)$, we first introduce a Schrödinger equation in which the imaginary part of the polarization potential of Eq. (25) is neglected. Namely,

$$\left[-\frac{\hbar^2}{2\mu}\left(\frac{d^2}{dr^2}-\frac{\ell(\ell+1)}{r^2}\right)+U_0+{\rm Re}\{V_{00,\ell}^{B\ {\rm pol}}\}-E\right]\Phi_{0,\ell}(k,r)=0. \tag{26}$$

We next introduce the ratio of the exact solution $\Psi_{0,\ell}(k,r)$ to the approximate solution $\Phi_{0,\ell}(k,r)$,

$$\beta_\ell(k,r)=\frac{\Psi_{0,\ell}(k,r)}{\Phi_{0,\ell}(k,r)}. \tag{27}$$

The functions $\Psi_{0,\ell}(k,r)$ and $\Phi_{0,\ell}(k,r)$ are related by a Lippmann-Schwinger equation involving the additional potential $\Delta V=-i\ {\rm Im}\{V_{00,\ell}^{B\ {\rm pol}}\}$ and the Green's function associated with Eq. (26). The transmission coefficient can be put in the form

$$T_\ell=\frac{8\mu}{k\hbar^2}\int_0^\infty dr|\beta_\ell(k,r)|^2|\Phi_{0,\ell}(k,r)|^2{\rm Im}\{U_0(r)\}. \tag{28}$$

At this point, we would like to analyze the behavior of the integrand in T_ℓ [Eq. (24)]. Since ${\rm Im}\{U_0\}$ represents fusion, one expects it to be of volume absorption nature with a rather sharp surface (small diffuseness). Further, the probability density $|\Psi_{0,\ell}(k,r)|^2$ is very much damped in the interior region, owing to strong absorption or centrifugal repulsion. Thus, the integrand should be sharply peaked at the strong absorption radius R_F. Similar arguments can be made if $\Psi_{0,\ell}$ is replaced by $\Phi_{0,\ell}$. This, in fact, we have numerically verified. It is thus safe to replace $|\beta_\ell(k,r)|^2$ by its value at $r=R_F$ and move it out of the integral. Therefore, one can write

$$T_\ell=|\beta_\ell(k,R_F)|^2\overline{T}_\ell, \tag{29}$$

where $\overline{T}_\ell$ is the transmission coefficient in the absence of ${\rm Im}\{V_{00,\ell}^{B\ {\rm pol}}\}$. Then, the CF cross section takes the form

$$\sigma_F=\frac{\pi}{k^2}\sum_{\ell=0}^{\infty}(2\ell+1)\overline{T}_\ell P_\ell^s, \tag{30}$$

where the factor

$$P^{s}_{\ell}=|\beta_{\ell}(k,R_F)|^2 \tag{31}$$

is the survival probability introduced in Ref. [1], which will be utilized in our applications in the following section. Now the major difference between $\Psi_{0,\ell}(R_F)$ and $\Phi_{0,\ell}(R_F)$ is the change in magnitude of the barrier reflected wave. Using the WKB argument of Takigawa *et al.* [2] one finds

$$\beta_{\ell}(k,R_F)=\exp\left[\frac{2}{\hbar v}\int_0^{\infty}dr|\Phi_{\ell}(k,r)|^2\mathrm{Im}\{V^{B\ \mathrm{pol}}_{00,\ell}(k,r)\}\right]. \tag{32}$$

Note that $\mathrm{Re}\{V^{B\ \mathrm{pol}}_{00,\ell}\}$ affects $\Phi_{0,\ell}$ through Eq. (26).

B. The incomplete fusion cross section

As we have shown in the previous section, the incomplete fusion cross section is given by Eqs. (21) and (22). These equations can be further simplified if we consider the contributions from each fragment, integrating over the degrees of freedom of the remaining one. Let us deal explicitly with Eq. (21), since extending the same treatment to Eq. (22) is straightforward. The incomplete fusion cross section can be written

$$\sigma_{\mathrm{IF}\,0}=\sigma^{c_1}_{\mathrm{IF}\,0}+\sigma^{c_2}_{\mathrm{IF}\,0}, \tag{33}$$

where

$$\sigma^{c_1}_{\mathrm{IF}\,0}=\frac{k}{E}\langle\Psi^{(+)}_0|V\hat{B}G^{(+)\dagger}_B\ \mathrm{Im}\{U_{c_1}\}G^{(+)}_B\hat{B}V|\Psi^{(+)}_0\rangle, \tag{34}$$

with a similar expression for $\sigma^{c_2}_{\mathrm{IF}\,0}$. Equation (34) can be put in a simpler form if one integrates over the degrees of freedom of fragment c_2. For this purpose, we should use the spectral representation of the Green's function in the space of this fragment. It is, however, more convenient to express it in terms of wave functions with ingoing scattered wave boundary conditions. From the identity $G^{(+)}_B\equiv G^{(-)\dagger}_B$, we get

$$G^{(-)\dagger}_B=\int\frac{d^3\mathbf{k}_2}{(2\pi)^3}|\chi^{(-)}_{\mathbf{k}_2})G^{(+)}_{c_1}(\tilde{\chi}^{(-)}_{\mathbf{k}_2}|. \tag{35}$$

Above, $\chi^{(-)}_{\mathbf{k}_2}$ and $\tilde{\chi}^{(-)}_{\mathbf{k}_2}$ are distorted waves for the motion of fragment c_2 satisfying the equations

$$[\varepsilon_{k_2}-h^{\mathrm{opt}}_{c2}]|\chi^{(-)}_{\mathbf{k}_2})=0,$$

$$[\varepsilon_{k_2}-(h^{\mathrm{opt}}_{c2})^{\dagger}]|\tilde{\chi}^{(-)}_{\mathbf{k}_2})=0, \tag{36}$$

and round brackets denote vectors in the space of this fragment. The operator

$$G^{(+)}_{c_1}=[\varepsilon_1-h^{\mathrm{opt}}_{c_1}]^{-1}, \tag{37}$$

with $\varepsilon_1=E-E_B-\varepsilon_{k_2}$ is a propagator acting exclusively on the degrees of freedom of fragment c_1.

Using Eqs. (35), its Hermitian conjugate and Eq. (37) in Eq. (34) we get

$$\sigma^{c_1}_{\mathrm{IF}\,0}=\frac{k}{E}\int\frac{d^3\mathbf{k}_2}{(2\pi)^3}\frac{d^3\mathbf{k}'_2}{(2\pi)^3}\times\langle\Psi^{(+)}_0|V\hat{B}|\chi^{(-)}_{\mathbf{k}'_2})G^{(+)\dagger}_{c_1}(\tilde{\chi}^{(-)}_{\mathbf{k}_2}|\tilde{\chi}^{(-)}_{\mathbf{k}'_2})\times\mathrm{Im}\{U_{c_1}\}G^{(+)}_{c_1}(\chi^{(-)}_{\mathbf{k}_2}|\hat{B}V|\Psi^{(+)}_0\rangle. \tag{38}$$

We now make the approximation

$$(\tilde{\chi}^{(-)}_{\mathbf{k}_2}|\tilde{\chi}^{(-)}_{\mathbf{k}'_2})=\delta(\mathbf{k}_2-\mathbf{k}'_2)-2i\frac{(\tilde{\chi}^{(-)}_{\mathbf{k}_2}|\mathrm{Im}\{U_{c_2}\}|\tilde{\chi}^{(-)}_{\mathbf{k}'_2})}{E_{k_2}-E_{k'_2}+i\epsilon}\approx\delta(\mathbf{k}_2-\mathbf{k}'_2), \tag{39}$$

which corresponds to taking the overlap integral to lowest order in $\mathrm{Im}\{U_{c_2}\}$. With this approximation, Eq. (38) becomes

$$\sigma^{c_1}_{\mathrm{IF}\,0}=\frac{k}{E}\int\frac{d^3\mathbf{k}'_2}{(2\pi)^3}\langle\Theta_{c_1,\mathbf{k}'_2}|\mathrm{Im}\{U_{c_1}(r_1)\}|\Theta_{c_1,\mathbf{k}'_2}\rangle, \tag{40}$$

where

$$|\Theta_{c_1,\mathbf{k}'_2}\rangle=G^{(+)}_{c_1}(\chi^{(-)}_{\mathbf{k}'_2}|\hat{B}V|\Psi^{(+)}_0\rangle=(\chi^{(-)}_{\mathbf{k}'_2}|G^{(+)}_{c_1}\hat{B}V|\Psi^{(+)}_0\rangle. \tag{41}$$

We have used the notation $|\Theta_{c_1,\mathbf{k}'_2}\rangle$ to emphasize that it is a vector in c_1 space, which depends also on the momentum of fragment c_2.

To simplify $|\Theta_{c_1,\mathbf{k}'_2}\rangle$, we rewrite the coupled-channel equation [Eqs. (2)] for $|\Psi_B\rangle$ neglecting the coupling to R space, in the form

$$[E-E_B-H^{\mathrm{opt}}_B]|\Psi^{(+)}_B\rangle=\hat{B}V|\Psi^{(+)}_0\rangle. \tag{42}$$

Plugging the result into Eq. (41), we get

$$|\Theta_{c_1,\mathbf{k}'_2}\rangle=G^{(+)}_{c_1}[E-E_B-\varepsilon_{k'_2}-h^{\mathrm{opt}}_{c_1}](\chi^{(-)}_{\mathbf{k}'_2}|\Psi^{(+)}_B\rangle. \tag{43}$$

Keeping in mind that $G^{(+)}_{c_1}\cdot[E-E_B-\varepsilon_{k'_2}-h^{\mathrm{opt}}_{c_1}]=1$ [see Eq. (37)] and using the coordinate space representation for clusters c_1 and c_2, we get

$$\Theta_{c_1,\mathbf{k}'_2}(\mathbf{r}_1)=\int d\mathbf{r}^3_2\chi^{(-)\dagger}_{\mathbf{k}'_2}\Psi^{(+)}_B(\mathbf{r}_1,\mathbf{r}_2). \tag{44}$$

To further reduce Eq. (40), we approximate the wave function $\Psi^{(+)}_B$ by the eikonal form [6]

$$\Psi^{(+)}_B(\mathbf{r}_1,\mathbf{r}_2)=A(\mathbf{k})\chi^{(+)}_{\mathbf{k}_1}(\mathbf{r}_1)\chi^{(+)}_{\mathbf{k}_2}(\mathbf{r}_2)\phi(\mathbf{r}_1-\mathbf{r}_2), \tag{45}$$

where $\mathbf{k}=\sqrt{2\mu E}/\hbar\hat{\mathbf{z}}$ is the incident wave vector and $\phi(\mathbf{r}_1-\mathbf{r}_2)$ is a short-range correlation arising from the interaction between the fragments. The wave vectors associated with the fragment motions $\mathbf{k}_1$ and $\mathbf{k}_2$ are given in terms of the breakup channel wave vector $\mathbf{k}'=\sqrt{2\mu(E-E_B)}/\hbar\hat{\mathbf{z}}$ as $\mathbf{k}_1=(m_{c_1}/m_a)\mathbf{k}'$ and $\mathbf{k}_2=(m_{c_2}/m_a)\mathbf{k}'$. The fragment distorted waves are

$$\chi^{(+)}_{\mathbf{k}_2}(\mathbf{r}_2)\equiv\chi^{(+)}_{\mathbf{k}_2}(\mathbf{b}_2,z_2)=e^{i\mathbf{k}_2\cdot r_2}\times\exp\left\{-i\frac{k_2}{2E_2}\int_{-\infty}^{z_2}dz_2' U_{c_2}(b_2,z_2')\right\} \quad (46)$$

and

$$\chi^{(-)*}_{\mathbf{k}_2'}(\mathbf{r}_2)\equiv\chi^{(-)*}_{\mathbf{k}_2'}(\mathbf{b}_2,z_2)=e^{-i\mathbf{k}_2'\cdot\mathbf{r}_2}\times\exp\left\{-i\frac{k_2'}{2E_2'}\int_{z_2}^{\infty}dz_2' U_{c_2}(b_2,z_2')\right\}. \quad (47)$$

The distorted waves for fragment c_1 are given by analogous expressions. In Eq. (45), $A(\mathbf{k})$ is a breakup probability amplitude, which was taken to be equal to the one in Ref. [6]. Using Eqs. (46) and (47) in Eq. (44), we get

$$\Theta_{c_1,\mathbf{k}_2'}(\mathbf{r}_1)=A(\mathbf{k})\chi^{(+)}_{\mathbf{k}_1}(\mathbf{r}_1)\int d^3\mathbf{r}_2 e^{i(\mathbf{k}_2-\mathbf{k}_2')\cdot\mathbf{r}_2}S_2(k_2b_2)\times\phi(\mathbf{r}_1-\mathbf{r}_2), \quad (48)$$

where $\mathbf{r}_2=\mathbf{b}_2+z\hat{\mathbf{z}}$ and

$$S_2(k_2b_2)=\exp\left\{-i\left[\frac{k_2'}{2E_2'}\int_{-\infty}^{z_2}dz' U_{c_2}(b_2,z')+\frac{k_2}{2E_2}\int_{z_2}^{\infty}dz' U_{c_2}(b_2,z')\right]\right\}\approx\exp\left\{-i\frac{k_2}{2E_2}\int_{-\infty}^{\infty}dz' U_{c_2}(b_2,z')\right\} \quad (49)$$

is the elastic S matrix for the scattering of the fragment c_2 from the target. The approximation involved in the obtention of Eq. (49) is the neglect of the Q value of the process. We now use the wave function of Eq. (48) to evaluate the incomplete fusion cross section [Eq. (40)]. We get

$$\sigma^{c_1}_{\mathrm{IF}\,0}=\frac{k}{E}\int d^3\mathbf{r}_1|A(\mathbf{k})\chi^{(+)}_{\mathbf{k}_1}(\mathbf{r}_1)|^2\mathrm{Im}\{U_{c_1}(r_1)\}F(\mathbf{k}_1,\mathbf{r}_1), \quad (50)$$

where

$$F(\mathbf{k}_1,\mathbf{r}_1)=\int d^3\mathbf{r}_2 d^3\mathbf{r}_2' S_2(k_2b_2)S_2^*(k_2b_2')\phi(\mathbf{r}_1-\mathbf{r}_2)\times\phi^*(\mathbf{r}_1-\mathbf{r}_2')\int\frac{d^3\mathbf{k}_2'}{(2\pi)^3}e^{i\mathbf{q}_2(\mathbf{r}_2-\mathbf{r}_2')}=\int d^3\mathbf{r}_2|S_2(k_2b_2)|^2|\phi(\mathbf{r}_1-\mathbf{r}_2)|^2. \quad (51)$$

Above, $F(\mathbf{k}_1,\mathbf{r}_1)$ plays the role of the survival probability of fragment c_2 averaged over the projectile extension. If we treat the projectile as a point particle (the effects of its finite size will be considered in the next section), namely take $\phi(\mathbf{r}_1-\mathbf{r}_2)\approx\delta(\mathbf{r}_1-\mathbf{r}_2)$, we get the simplification $F(\mathbf{k}_1,\mathbf{r}_1)=|S_2(k_2b_1)|^2$ and, using the eikonal form for $\chi^{(+)}_{\mathbf{k}_1}(\mathbf{r}_1)$ [Eq. (46)], the incomplete fusion cross section becomes

$$\sigma^{c_1}_{\mathrm{IF}\,0}=\frac{k}{E}\int d^2\mathbf{b}_1|A(\mathbf{k})|^2|S_2(k_2b_1)|^2\times\int_{-\infty}^{\infty}dz_1\ \mathrm{Im}\{U_{c_1}(b_1,z_1)\}\times\exp\left\{-\frac{k_1}{E_1}\int_{-\infty}^{z_1}dz_1'\ \mathrm{Im}\{U_{c_1}(b_1,z_1')\}\right\}. \quad (52)$$

The integration over z_1 is straightforward and we get

$$\sigma^{c_1}_{\mathrm{IF}\,0}=\frac{kE_1}{k_1E}\int d^2\mathbf{b}_1|A(\mathbf{k})|^2|S_2(k_2b_1)|^2(1-|S_1(k_1b_1)|^2). \quad (53)$$

The accuracy of the above expression at low collision energies can be improved if one converts the impact parameter to a partial wave, according to the usual prescription. Namely,

$$\begin{aligned} bk_1&\to(\ell_1+1/2), \quad \int d^2\mathbf{b}_1\to\frac{\pi}{k_1^2}\sum_{\ell_1}(2\ell_1+1),\\ bk_2&\to(\ell_2+1/2),\\ bk&\to(\ell_0+1/2). \end{aligned} \quad (54)$$

Equation (53) then becomes

$$\sigma^{c_1}_{\mathrm{IF}\,0}=\left(\frac{v'}{v}\right)\frac{\pi}{k_1^2}\sum_{\ell_1}(2\ell_1+1)\times(1-|S_1(\ell_1,E_1)|^2)|A(\ell_0)|^2|S_2(\ell_2,E_2)|^2, \quad (55)$$

where $v'=\hbar k'/\mu$ and $v=\hbar k/\mu$.

Introducing the transmission coefficient for fragment c_1 $T^{(1)}_{\ell_1}(E_1)$ the breakup probability $P^B_{\ell_0}(E)$ and the survival probability for fragment c_2 $[1-T^{(2)}_{\ell_2}(E_2)]$ given by

$$\begin{aligned} P^B_{\ell_0}(E)&=|A(\ell_0)|^2,\\ T^{(1)}_{\ell_1}(E_1)&=(1-|S_1(\ell_1,E_1)|^2),\\ [1-T^{(2)}_{\ell_2}(E_2)]&=|S_2(\ell_2,E_2)|^2, \end{aligned} \quad (56)$$

Eq. (55) takes the final form

$$\sigma^{c_1}_{\mathrm{IF}\,0}=\left(\frac{v'}{v}\right)\overline{\sigma}^{c_1}_{\mathrm{IF}\,0}, \quad (57)$$

with

$$\overline{\sigma}^{c_1}_{\mathrm{IF}\,0}=\frac{\pi}{k_1^2}\sum_{\ell_1}(2\ell_1+1)T^{(1)}_{\ell_1}(E_1)P^B_{\ell_0}(E)[1-T^{(2)}_{\ell_2}(E_2)]. \quad (58)$$

1. Effect of the finite nuclear size on incomplete fusion

In this subsection we drop the approximations of infinite target mass and of a pointlike projectile. In the previous section, the angular momentum of fragment c_2 was determined

from ℓ_1 through the relation $\ell_2=(k_2/k_1)\ell_1$. In a projectile with finite extension, the impact parameters of the two fragments are no longer the same and a given ℓ_1 value leads to a distribution $W(\ell_1,\ell_2)$ for the angular momentum of fragment c_2. As we will see below, this distribution can be determined from the wave funcion describing the fragment motion inside the projectile. Furthermore, if the target mass is finite, one has to be careful to write the angular momenta in the appropriate coordinate frame. If one intends to employ stardard results for the cross section of Eq. (58), the angular momenta ℓ_1, ℓ_2, and ℓ_0 should be given in the c_1-target, c_2-target, and projectile-target rest frames, respectively. On the other hand, given the angular momenta ℓ_1 and ℓ_2 of the two fragments, the angular momentum of the projectile center of mass ℓ_0 is uniquely determined. If we find the distribution $W(\ell_1,\ell_2)$, the cross section of Eq. (58) can be written as

$$\overline{\sigma}^{c_1}_{\mathrm{IF}\,0}=\frac{\pi}{k_1^2}\sum_{\ell_1}(2\ell_1+1)\langle P^{c_1}_{\ell_1}\rangle, \tag{59}$$

with

$$\langle P^{c_1}_{\ell_1}\rangle=T^{(1)}_{\ell_1}(E_1)\sum_{\ell_2}W(\ell_1,\ell_2)P^{B}_{\ell_0(\ell_1,\ell_2)}(E)\times[1-T^{(2)}_{\ell_2}(E_2)]. \tag{60}$$

Above, the average is taken with respect to the possible values of the angular momentum ℓ_2 for a given ℓ_1 and the notation $P^B_{\ell_0(\ell_1,\ell_2)}$ is used to stress the fact that ℓ_0 is a function of ℓ_1 and ℓ_2. Of course, one must have

$$\sum_{\ell_2}W(\ell_1,\ell_2)=1 \quad \text{for any } \ell_1. \tag{61}$$

In order to determine $W(l_1,l_2)$, we first consider the impact parameters associated to the corresponding orbital angular momenta $b_i=l_i/k_i$ $(i=1,2)$, where $k_i=\sqrt{2\mu_i E_i}/\hbar$, $\mu_i=m_i m_T/(m_i+m_T)$, and $E_i=\mu_i\sqrt{E-E_B}/\mu$ is the energy of the c_i-target motion considered in the c.m. frame of this system and B is the breakup energy. The probability distribution $W(\ell_1,\ell_2)$ then leads to a probability density $w(b_1,b_2)$. Notice that $w(b_1,b_2)$ is a differential probability, since the impact parameters b_2 is a continous variable. To calculate $w(b_1,b_2)$, we assume that the wave function for the separation between the two fragments is Gaussian, so that their separation $\mathbf{r}_1-\mathbf{r}_2$ has the distribution

$$P(\mathbf{r}_1-\mathbf{r}_2)\equiv|\phi(\mathbf{r}_1-\mathbf{r}_2)|^2=A\,\exp\left[-\left(\frac{\mathbf{r}_1-\mathbf{r}_2}{\alpha}\right)^2\right], \tag{62}$$

where α is a typical length of the fragment distribution and $A=1/(\alpha\sqrt{\pi})^3$ is a normalization constant. Expressing $\mathbf{r}_1$ and $\mathbf{r}_2$ in terms of cylindrical coordinates $(b_1,\varphi_1,z_1;b_2,\varphi_2,z_2)$ and integrating $P(\mathbf{r}_1-\mathbf{r}_2)$ over z_2 and φ_2, we get

$$w(b_1,b_2)=\int dz_2 d\varphi_2 P(\mathbf{r}_1-\mathbf{r}_2)=\frac{2}{\alpha^2}\exp\left[-\frac{(b_1-b_2)^2}{\alpha^2}\right]\overline{I}_0(t), \tag{63}$$

where $t=2b_1b_2/\alpha^2$ and $\overline{I}_0$ is related to the standard modified Bessel function I_0 through $\overline{I}_0(t)=e^{-t}I_0(t)$.

From the impact parameter distribution $w(b_1,b_2)$ we can switch to the angular momentum distribution. We first replace $b_i=l_i/k_i$, $i=1,2$, take integer values for l_1, and then find $W(l_1,l_2)$ through the semiclassical prescription

$$W(l_1,l_2)=\int_{l_2-1/2}^{l_2+1/2}w(l_1/k_1,\lambda_2/k_2)\lambda_2 d\lambda_2. \tag{64}$$

In the case $l_2=0$ the lower integration limit must be taken equal to zero, and the final distribution for each value of l_1 must be normalized according to Eq. (61).

From l_1 and l_2 we may determine the orbital angular momentum of the projectile-target system in their c.m. frame l_0 as the nearest integer to the semiclassical value

$$\left(\frac{m_1+m_T}{m_P+m_T}\right)l_1+\left(\frac{m_2+m_T}{m_P+m_T}\right)l_2. \tag{65}$$

2. Inclusion of the breakup energy distribution

Let us now estimate the effect of the kinetic energy associated to the relative motion between projectile fragments on the incomplete fusion cross section. For simplicity, we consider the contribution arising from the fusion of fragment c_1 with the target through the coupling with the ground state of the projectile. The contribution from fragment c_2 as well as the effects of the coupling with the excited state R can be evaluated in a similar way. We take as a starting point the momentum probability distribution corresponding to the Fourier transform of $P(\mathbf{r}_1-\mathbf{r}_2)$ [Eq. (62)], approximated by the Gaussian

$$\frac{dP(\mathbf{p})}{d^3\mathbf{p}}=N'\,\exp\left(-\frac{p^2}{p_0^2}\right), \tag{66}$$

where $\mathbf{p}$ is the relative momentum between the two fragments and $p_0=\hbar/\alpha$. Equation (66) is basically the distribution used in Ref. [7]. This distribution gives rise to the dissociation energy spectrum in the projectile frame

$$\frac{dP(\varepsilon)}{d\varepsilon}=N\sqrt{\frac{\varepsilon}{\varepsilon_0}}\exp\left(-\frac{\varepsilon}{\varepsilon_0}\right). \tag{67}$$

In Eqs. (66) and (67), p_0 and and ε_0 are parameters of the distribution to be determined from the experimental dissociation spectra and N' and N are appropriate normalization constants.

This dissociation energy spectrum leads to a dispersion of the fragment energy E_1' around the value E_1 appearing in Eqs. (57) and (58). This distribution is given by

$$\frac{dP}{dE_1'}=\langle\delta[E_1'-E_1(\mathbf{p})]\rangle=N'\int e^{-(p/p_0)^2}\delta[E_1'-E_1(\mathbf{p})]d^3\mathbf{p}, \tag{68}$$

where $E_1(\mathbf{p})$ is the fragment kinetic energy in the c.m. of the fragment-target frame when the relative momentum of the fragments is $\mathbf{p}$. In this way we obtain the distribution

$$\frac{dP}{dE_1'} = C[e^{-(\sqrt{E_1'}-\sqrt{E_1})^2/\Delta_1} - e^{-E_1/\Delta_2}], \quad \text{for} \quad \frac{\left(\sqrt{E_1'}-\sqrt{E_1}\right)^2}{\Delta_1} \leqslant \frac{E_1}{\Delta_2}$$

$$= 0, \quad \text{otherwise}, \tag{69}$$

where C is a normalization constant and Δ_1 and Δ_2 are related to the parameter ε_0 of Eq. (67) as

$$\Delta_1 = \frac{m_T m_2}{m_P(m_T+m_1)}\varepsilon_0, \tag{70}$$

$$\Delta_2 = \frac{m_1(m_P+m_T)}{m_P(m_T+m_1)}\varepsilon_0. \tag{71}$$

The contribution from fragment c_1 to the incomplete fusion cross section is obtained averaging Eq. (57) with the above distribution. Namely,

$$\sigma_{\rm IF}^{c_1}(E_1) = \int \sigma_{\rm IF}^{c_1}(E_1')\left[\frac{dP}{dE_1'}\right]dE_1'. \tag{72}$$

Notice that in the absence of Fermi motion the distribution dP/dE_1' becomes proportional to a δ function and one recovers the result of the previous section.

IV. APPLICATIONS

In this section we calculate the complete and incomplete fusion cross sections for the collision of ^{6}Li and ^{9}Be projectiles on a ^{12}C target. These systems have some interesting features. First, the thresholds for projectile breakup are $B(^6\text{Li}\rightarrow{}^2d+\alpha)=1.47$ MeV, $B(^9\text{Be}\rightarrow n+{}^8\text{Be})=1.65$ MeV, which are extremely low in comparison to that for the breakup of a typical heavy ion ($\approx$10 MeV). In this sense, these collisions behave in a manner similar to reactions involving nuclei far from the stability line. Second, the dissociation energies are not negligible compared to the Coulomb barrier, which may lead to important threshold effects for incomplete fusion. This can be seen in Eq. (55) where the transmission coefficient $[1-|S(\ell_1,E_1)|^2]$ vanishes below the threshold $E_1<(E-E_B)\mu_1/\mu$.

To handle the complete and incomplete fusion processes under the same footing, we treat the nuclear interaction in both cases in a consistent way [8]: we consider a standard double-folding calculation of the nuclear potential. We employ the $M3Y$ force [9] and take nuclear densities from experiment [10] to construct the optical potentials for projectile target and fragment target. From the total (nuclear + Coulomb + centrifugal) optical potentials $V_l^{(i)}(r)$ we determine the transmission coefficients for each partial wave. At sub-barrier energies, these coefficients are calculated using the improved WKB approximation

$$T_l^{(i)}(E_i) = \frac{1}{1+\exp[\Theta_l^{(i)}(E_i)]}, \tag{73}$$

where

$$\Theta_l^{(i)}(E_i) = 2\int_{r_1}^{r_2}\frac{\sqrt{2\mu_i[E_i - V_l^{(i)}(r)]}}{\hbar}dr \tag{74}$$

is the penetrability factor, with r_1 and r_2 the inner and outer turning points. At energies above the barrier we take the Hill-Wheeler expression $\Theta_l^{(i)}(E_i)=2\pi(V_{B,l}^{(i)}-E_i)/\hbar\omega_l^{(i)}$, where $V_{B,l}^{(i)}$ and $\omega_l^{(i)}$ are the height and curvature of the effective barrier for the interaction between fragment i and the target at the lth partial wave. We should remark that, although satisfactory for a qualitative view of the problem, one should not expect that this general treatment of the nuclear potential gives an accurate description of the fusion barrier and, consequently, of the fusion cross section. One should keep in mind that we are dealing with very light nuclei, for which details of their structure may bring about important changes in their interaction.

The breakup probabilities appearing in the incomplete fusion cross sections and also in the survival probabilities are given in Refs. [11,1,4]. They can be written

$$P_l^{\rm bu}(E) = 1-\exp\left[-\frac{2\mathcal{F}_0^2}{E(E-B)}|S_l(E-B)|I_l^2(\eta,s,\xi)\right], \tag{75}$$

where $|S_l(E-B)|^2 \approx 1-T_l^{(0)}(E-B)$ is the absolute value of the l-projected optical S matrix for a collision initiated in the elastic channel with energy $E-B$. The Coulomb radial integral $I_l(\eta,s,\xi)$ is given by

$$I_l(\eta,s,\xi) = \int_0^\infty F_l(\eta,k,r)F_l(\eta',k',r)e^{-r/\alpha}dr. \tag{76}$$

Above, η, k (η', k') are, respectively, the entrance channel values of the Sommerfeld parameter and the wave number for the collision energy E (collision energy E'). $\alpha = \sqrt{2\mu_P B}/\hbar$, where $\mu_P = m_0 A_i(A_p-A_i)/A_p$ is the characteristic length of the fragment orbit within the projectile, $s = 1/(k\alpha)$, and $\xi=(k-k')/(k+k')$. In Eq. (75), $\mathcal{F}_0$ is the strength of the breakup form factor. Since it depends strongly on the projectile-target system and on the collision energy range, it should be fitted to the experimental situation under study. If one knows this quantity for a given projectile P and target T at near barrier energies, it can be estimated for a different target T' through the scaling rule [11]

$$\mathcal{F}_0(T') = \mathcal{F}_0(T)e^{(R_{T'}-R_T)/\alpha}. \tag{77}$$

It should be noted that in the present calculation we neglect the real part of the polarization potential, as in Ref. [11]. This part vanishes within the on-energy-shell approximation for the Green's function. However, it is likely that it becomes relevant at sub-barrier energies leading to a lower effective barrier and enhancing the fusion cross section [3].

We used the above results to study complete and incomplete fusion in the collision ^{6}Li+^{12}C. In this case, incom-

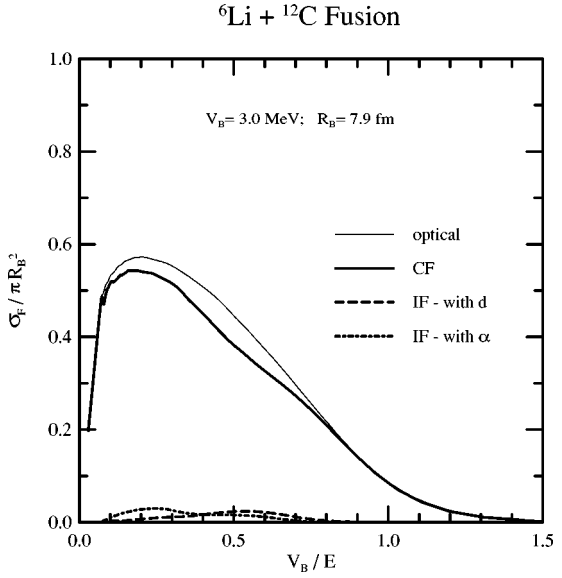

FIG. 1. The complete and incomplete fusion cross sections for the system ^{6}Li+^{12}C, normalized to the asymptotic value πR_B^2. See the text for details.

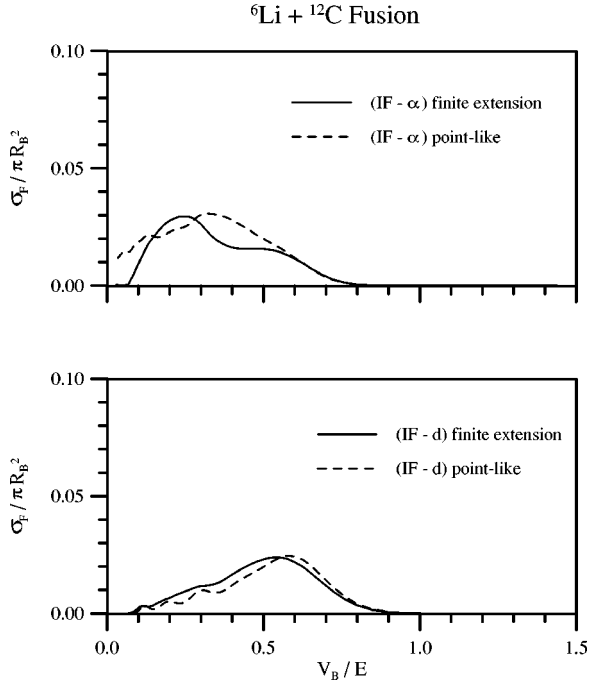

FIG. 2. Effect of the finite extension of the projectile fragments on the incomplete fusion cross sections for the system ^{6}Li+^{12}C.

plete fusion corresponds to the fusion of the ^{12}C target with one of the fragments (d or α) produced in the projectile dissociation. The breakup of ^{12}C can be neglected due to its large dissociation energy.

In Fig. 1, we show the complete and incomplete fusion cross sections for the collision ^{6}Li+^{12}C. The contributions from d and α to incomplete fusion are plotted separately. In the calculation, we have used the strength $\mathcal{F}_0 = 5.0$ MeV, which is of the order of those used in Ref. [4] for similar systems. As we can see, at sub-barrier energies ($V_B/E > 1$) the effect of breakup on $\sigma_{\rm CF}$ is negligible. However, at higher energies, incomplete fusion becomes appreciable and complete fusion starts deviating from the one-dimensional optical prediction. It is interesting to note that the incomplete fusion corresponding to the capture of the deuteron dominates over that of the α particle at energies below 2.5 V_B, while the situation is reversed above this energy. These trends depend on the share of the incident energy carried by each fragment and on the fragment charge. Optimal conditions for sub-barrier and near-barrier fusion are a large ratio μ_i/μ and a small ratio Z_i/Z_p. It can be easily checked that the deuteron fragment is favored by this criterion. Therefore, the fusion with deuteron is enhanced at lower impact energies, in comparison to that of the α particle. At higher energies, this effect becomes negligible and the larger spacial extent of the α particle, as reflected in the Coulomb barrier radius, predominates. It should be mentioned that the corresponding results presented in the preliminary calculations of Ref. [8] are somewhat different. The discrepancies have two origins. The first is that in the present calculation we use a $M3Y$ interaction strength which is suitable for low-energy applications. The second is that in Ref. [8] we made the crude approximation of neglecting the differences among the angular momenta ℓ_0, ℓ_1, and ℓ_2. This approximation leads to appreciable differences in the incomplete fusion cross sections.

In Fig. 2 we show the effect of the pointlike approximation and in Fig. 3 that of the Fermi motion on the incomplete fusion cross section induced by the α-particle and deuteron fragments. We notice that, especially in the case of the α particle, the former approximation is important at high energies while the Fermi motion effects are dominant at low energies, extending into the sub-barrier region.

Figures 4–6 illustrate the results for the case of an incident ^{9}Be projectile. In this case we did not consider the incomplete fusion process induced by the neutron, except through its hindrance on the ^{8}Be fragment incomplete fusion cross section. The results are qualitatively similar, although the incomplete fusion process is more important than in the ^{6}Li case at large collision energies.

Comparison with experiment. In this section we compare theoretical predictions of the present theory with experimental data. Although there are no available data on incomplete fusion for the systems considered in the previous section, there are some data on the complete fusion of ^{6}Li+^{12}C. For a quantitative description of the corresponding cross section, the use of a general potential, such as the one in the previous section, would not be appropriate. One should use a potential that could lead to an accurate fusion barrier in the absence of breakup. Breakup effects could then be taken into account through the inclusion of survival probabilities, as in Eq. (30). In the ^{6}Li+^{12}C case, it is possible to find such a fusion barrier from the CF data of the ^{7}Li+^{12}C collision. These two systems are nearly identical in the entrance channel. However, the ^{7}Li breakup energy (into an α particle and ^{3}H) is about 1 MeV larger than that for ^{6}Li. Since the breakup probability depends critically on the breakup energy [12], it is reasonable to neglect breakup in the ^{7}Li+^{12}C case. Therefore, this system can be seen as ^{6}Li+^{12}C with breakup ''switched off.''

An appropriate fit of the optical potential to the ^{7}Li +^{12}C CF data requires a fully quantal treatment (rather than the simple WKB tunneling with infinite short-range volume

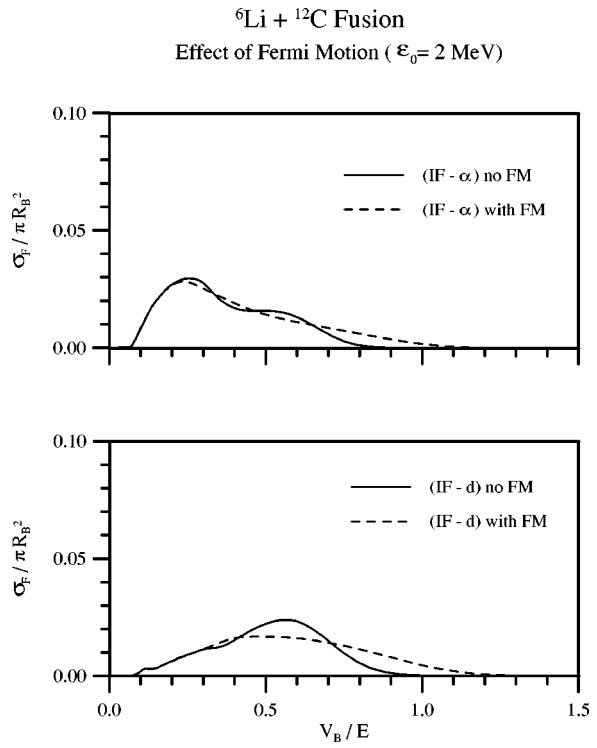

FIG. 3. Effect of Fermi motion on the incomplete fusion cross sections for the system ^{6}Li+^{12}C.

absorption) and should include surface absorption. Instead of carrying out this procedure, we follow the simpler approach used by Takahashi *et al.* [4]. First, we parametrize the fusion barrier [13] in terms of its height V_b, radius R_b, and curvature $\hbar\omega$. In addition, we introduce a cutoff in the partial wave summation at the angular momentum $\hbar L_{\rm crit}$. This parameter depends on the entrance channel and also on the details of the compound nucleus produced in the complete fusion process. V_b, R_b, $\hbar\omega$, and $L_{\rm crit}$ are then fitted to reproduce the CF data in the ^{7}Li+^{12}C collision. Using the same barrier parameters and including a survival probability for each partial wave, one then obtains the CF cross section

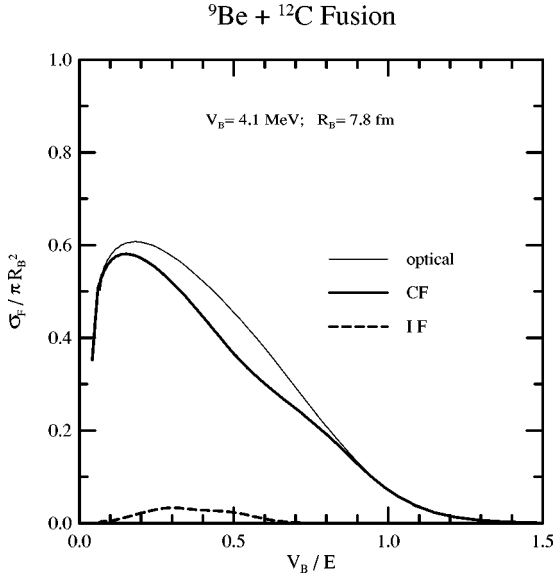

FIG. 4. Similar to Fig. 1 for the system ^{9}Be+^{12}C.

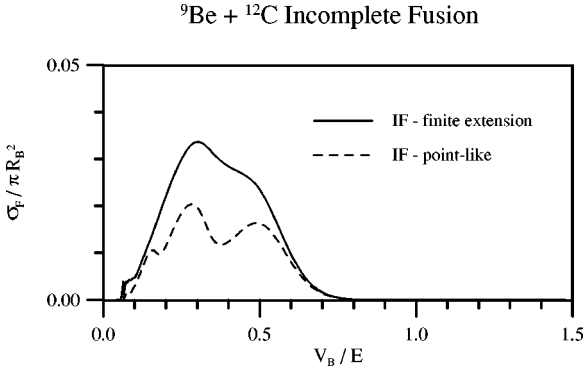

FIG. 5. Similar to Fig. 2 for the system ^{9}Be+^{12}C.

for the ^{6}Li+^{12}C collision. In Ref. [4] this procedure was followed for these collisions and also for ^{7}Li+^{9}Be and ^{6}Li +^{9}Be. The agreement between theory and experiment was quite good. For illustration, we use here the same approach for ^{6}Li+^{12}C. In Fig. 7(a), the experimental CF cross section for ^{7}Li+^{12}C is compared to the parametrized cross section for V_b=4.14 MeV, R_b=6.32 fm, $\hbar\omega$=3.31 MeV, and for the cutoff angular momentum it is $L_{\rm crit}=10\hbar$. The fit is quite good. Since V_b, R_b, and $\hbar\omega$ depend exclusively on the entrance channel, it is safe to use the same values for the fusion barrier in the ^{6}Li+^{12}C system.

The results for ^{6}Li+^{12}C are shown in Fig. 7(b), in comparison with the data. The agreement is good, indicating that breakup effects in $\sigma_{\rm CF}$ can be taken into account through the survival probability discussed in the previous sections. We should mention that it was necessary to use a different critical angular momentum $L_{\rm crit}=8$. Since $L_{\rm crit}$ depends on the details of the compound nucleus, which are rather different in these two cases, this situation is not surprising.

V. CONCLUSIONS

In the present paper, we developed a model that allows the study of the competition between fusion and breakup of a rather weakly bound two-cluster nucleus impinging on a target. Starting from the coupled-channel equations, we obtain expressions for complete and incomplete fusion cross sections. The expression for $\sigma_{\rm CF}$ containing a survival probability factor which has been assumed in a previous paper [1] was formally derived. The effects of the final extension of the projectile and also of the fragment Fermi motion inside

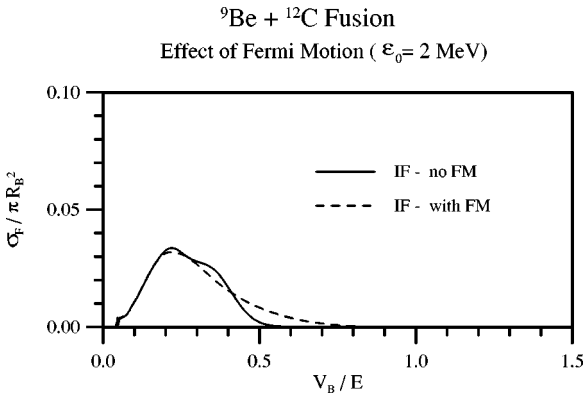

FIG. 6. Similar to Fig. 3 for the system ^{9}Be+^{12}C.

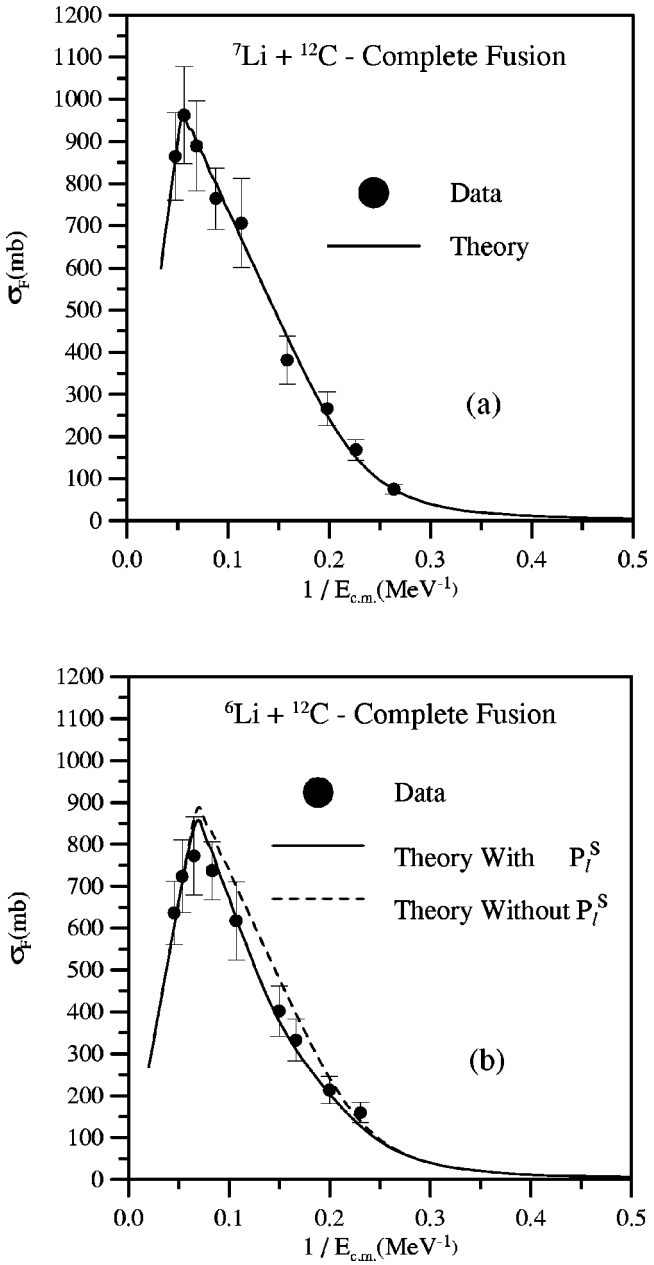

FIG. 7. Experimental and theoretical cross sections for complete fusion in the collisions (a) ^{7}Li+^{12}C and (b) ^{6}Li+^{12}C. The data are from Takahashi *et al.* [4]. For details, see the text.

the projectile have been assessed.

It is important to emphasize that although in the present work we have discussed at length the effect of the breakup channel on the complete fusion cross section, our theory permits the inclusion of other couplings, our subspace R, that would result in the well-known phenomenon of the enhancement of complete fusion at sub-barrier energies. It also allows similar enhancement in the incomplete fusion cross section.

The model was used to study the complete fusion of ^{6}Li and ^{9}Be projectiles with a ^{12}C target nucleus. The complete fusion cross section is found to be significantly hindered at energies $E \geqslant 1.5V_B$. At slightly higher energies, the total fusion cross section is also smaller than that in the no-coupling limit. The incomplete fusion cross sections were shown to be smaller than those corresponding to complete fusion for both systems considered. However, at large energies they should be easily measurable. These findings are of great relevance to the fusion of halo nuclei such as ^{11}Li and ^{11}Be.

ACKNOWLEDGMENTS

We would like to acknowledge partial financial support from the MCT/FINEP/CNPq (PRONEX) under Contract No. 41.96.0886.00, the Fundação de Amparo à Pesquisa do Estado do Rio de Janeiro (FAPERJ), the Fundação de Amparo à Pesquisa do Estado de São Paulo (FAPESP) under Contract No. 96/1381-0, and the Fundação Universitária José Bonifácio.

APPENDIX: THE IMAGINARY PART OF AN ABSORPTIVE GREEN'S FUNCTION

In this appendix we derive a general formal expression for the imaginary part of the Green's function that describes the propagation of a particle in a complex optical potential

$$G^{(+)}(E)=\frac{1}{E-H_0-U+i\epsilon}, \tag{A1}$$

where H_0 is the Hermitian kinetic energy operator and U is taken to be non-Hermitian ($U^\dagger \neq U$). We write now the inverse of $G^{(+)}$

$$[G^{(+)}(E)]^{-1}=E-H_0-U+i\epsilon \tag{A2}$$

and its complex conjugate

$$[G^{(+)}(E)]^{-1^\dagger}=E-H_0-U^\dagger-i\epsilon. \tag{A3}$$

The difference between Eqs. (A2) and (A3) is then

$$\begin{aligned}[G^{(+)}(E)]^{-1^\dagger}-[G^{(+)}(E)]^{-1}&=U-U^\dagger-2i\epsilon\\&=U-U^\dagger+[G_0^{(+)}(E)]^{-1^\dagger}-[G_0^{(+)}(E)]^{-1},\end{aligned} \tag{A4}$$

where we have introduced the free propagator

$$G_0^{(+)}(E)=\frac{1}{E-H_0+i\epsilon}. \tag{A5}$$

Multiplying Eq. (A4) on the right by $G^{(+)}(E)$ and on the left by $G^{(+)^\dagger}(E)$ we obtain

$$\begin{aligned}G^{(+)}(E)-G^{(+)}(E)^\dagger&=G^{(+)}(E)^\dagger(U-U^\dagger)G^{(+)}(E)+G^{(+)}(E)^\dagger\\&\quad\times[G_0^{(+)}(E)^{-1^\dagger}-G_0^{(+)}(E)^{-1}]G^{(+)}(E).\end{aligned} \tag{A6}$$

We now use the Lippman-Schwinger representation for $G^{(+)}$ and $G^{(+)^\dagger}$

$$\begin{aligned}G^{(+)}(E)&=G_0^{(+)}+G_0^+UG^{(+)}(E)=G_0^{(+)}[1+UG^{(+)}(E)]\\G^{(+)}(E)^\dagger&=G_0^{(+)}(E)^\dagger+G^{(+)}(E)^\dagger U^\dagger G_0^{(+)^\dagger}\\&=(1+G^{(+)^\dagger}U^\dagger)G_0^{(+)^\dagger}.\end{aligned} \tag{A7}$$

Employing Eq. (A7) in the second term on the RHS of Eq. (A6), we obtain finally

$$G^{(+)}(E)-G^{(+)}(E)^{\dagger} = G^{(+)}(E)^{\dagger}(U-U^{\dagger})G^{(+)}(E)+\Omega^{(-)}(E) \times[G_0^{(+)}(E)-G_0^{(+)}(E)^{\dagger}]\Omega^{(-)}(E)^{\dagger}, \quad \text{(A8)}$$

where we have introduced the Møller operators $\Omega^{(-)}(E)=[1+G^{(+)^{\dagger}}U^{\dagger}]$ which when used transforms the plane wave into an ingoing distorted wave:

$$\Omega^{(-)}(E)|\vec{k}\rangle=|\chi_{\vec{k}}^{(-)}\rangle, \quad \text{(A9)}$$

which is a solution of the dual Schrödinger equation

$$(E_k-H_0-U^{\dagger}-i\epsilon)|\chi_k^{(-)}\rangle=0. \quad \text{(A10)}$$

Equation (A8) is the desired relation which is employed to obtain Eq. (8). Notice that $G^{(+)}(E)^{\dagger}=G^{(-)}(E)$. For more details concerning scattering theory for non-Hermitian potentials see Ref. [14].

[1] M. S. Hussein, M. P. Pato, L. F. Canto, and R. Donangelo, Phys. Rev. C **46**, 377 (1992).

[2] N. Takigawa, M. Kuratani, and H. Sagawa, Phys. Rev. C **47**, R2470 (1993).

[3] C. H. Dasso and A. Vitturi, Phys. Rev. C **50**, R12 (1994).

[4] J. Takahashi, M. Munhoz, E. M. Szanto, N. Carlin, N. Added, A. A. P. Suaide, M. M. Moura, R. Liguori Neto, A. Szanto de Toleto, and L. F. Canto, Phys. Rev. Lett. **78**, 30 (1997).

[5] M. S. Hussein, R. A. Rego, and C. A. Bertulani, Phys. Rep. **201**, 279 (1991).

[6] M. S. Hussein and K. W. McVoy, Nucl. Phys. **A445**, 124 (1985).

[7] A. S. Goldhaber, Phys. Lett. **53B**, 306 (1974).

[8] L. F. Canto, R. Donangelo, M. S. Hussein, and P. Lotti, J. Phys. G **23**, 1465 (1997).

[9] G.F. Bertsch, J. Borysowicz, H. McManus, and W. G. Love, Nucl. Phys. **A284**, 399 (1977); A. M. Kobos, B. A. Brown, R. Lindsay, and G. R. Satchler, *ibid.* **A425**, 205 (1984).

[10] H. de Vries H, C. W. de Jager, and C. de Vries, At. Data Nucl. Data Tables **36**, 495 (1987).

[11] L. F. Canto, R. Donangelo, M. S. Hussein, and M. P. Pato, Nucl. Phys. **A542**, 131 (1992).

[12] J. Takahashi, Ph.D. thesis, Instituto de Física–Universidade de São Paulo, SP-Brasil, 1995.

[13] D. Glas and U. Mosel, Nucl. Phys. **A237**, 429 (1975).

[14] M. S. Hussein, Ann. Phys. (N.Y.) **175**, 197 (1987); **177**, 58 (1987).